

## ANESTHESIOLOGY

# Early Postnatal Exposure to Isoflurane Disrupts Oligodendrocyte Development and Myelin Formation in the Mouse Hippocampus

Qun Li, Ph.D., Reilley P. Mathena, B.S.,  
Jing Xu, M.D., O'Rukevwe N. Eregha, B.A.,  
Jieqiong Wen, B.S., Cyrus D. Mintz, M.D., Ph.D.

*ANESTHESIOLOGY* 2019; 131:1077–91

## EDITOR'S PERSPECTIVE

### What We Already Know about This Topic

- Oligodendrocyte proliferation and maturation are prerequisites for myelination in the central nervous system. Disruption of these processes can lead to long-term impairment of neural function.
- Laboratory models demonstrate a variety of effects of anesthetics on the immature brain, but the consequences of early life anesthesia exposure on oligodendrocyte development have not been previously reported.

### What This Article Tells Us That Is New

- Exposure of 7-day-old mouse pups to isoflurane (1.5%, 4 h) results in lasting impairments of oligodendrocyte proliferation and differentiation.
- These effects lead to defects in myelinations and are associated with cognitive dysfunction.
- The underlying molecular mechanisms involve the isoflurane-induced activation of the mammalian target of rapamycin pathway and a related decrease in DNA methylation in oligodendrocyte progenitors.

Modern general anesthesia allows the safe performance of several hundred million surgical procedures annually.<sup>1</sup> However, there is growing concern that some vulnerable categories of patients, particularly young

## ABSTRACT

**Background:** Early postnatal exposure to general anesthetics may interfere with brain development. We tested the hypothesis that isoflurane causes a lasting disruption in myelin development *via* actions on the mammalian target of rapamycin pathway.

**Methods:** Mice were exposed to 1.5% isoflurane for 4 h at postnatal day 7. The mammalian target of rapamycin inhibitor, rapamycin, or the promyelination drug, clemastine, were administered on days 21 to 35. Mice underwent Y-maze and novel object position recognition tests ( $n = 12$  per group) on days 56 to 62 or were euthanized for either immunohistochemistry ( $n = 8$  per group) or Western blotting ( $n = 8$  per group) at day 35 or were euthanized for electron microscopy at day 63.

**Results:** Isoflurane exposure increased the percentage of phospho-S6-positive oligodendrocytes in fimbria of hippocampus from  $22 \pm 7\%$  to  $51 \pm 6\%$  ( $P < 0.0001$ ). In Y-maze testing, isoflurane-exposed mice did not discriminate normally between old and novel arms, spending equal time in both ( $50 \pm 5\%$  old: $50 \pm 5\%$  novel;  $P = 0.999$ ), indicating impaired spatial learning. Treatment with clemastine restored discrimination, as evidenced by increased time spent in the novel arm ( $43 \pm 6\%$  old: $57 \pm 6\%$  novel;  $P < 0.001$ ), and rapamycin had a similar effect ( $44 \pm 8\%$  old: $56 \pm 8\%$  novel;  $P < 0.001$ ). Electron microscopy shows a reduction in myelin thickness as measured by an increase in g-ratio from  $0.76 \pm 0.06$  for controls to  $0.79 \pm 0.06$  for the isoflurane group ( $P < 0.001$ ). Isoflurane exposure followed by rapamycin treatment resulted in a g-ratio ( $0.75 \pm 0.05$ ) that did not differ significantly from the control value ( $P = 0.426$ ). Immunohistochemistry and Western blotting show that isoflurane acts on oligodendrocyte precursor cells to inhibit both proliferation and differentiation. DNA methylation and expression of a DNA methyl transferase 1 are reduced in oligodendrocyte precursor cells after isoflurane treatment. Effects of isoflurane on oligodendrocyte precursor cells were abolished by treatment with rapamycin.

**Conclusions:** Early postnatal exposure to isoflurane in mice causes lasting disruptions of oligodendrocyte development in the hippocampus *via* actions on the mammalian target of rapamycin pathway.

(*ANESTHESIOLOGY* 2019; 131:1077–91)

children, geriatric patients, and individuals with underlying brain disorders, may be at risk of lasting cognitive dysfunction.<sup>2–4</sup> While conclusive evidence of anesthetic neurotoxicity has not been established in human studies, some animal studies have shown that exposure to general anesthetics in early development causes impaired neurocognitive performance<sup>5–8</sup> and that the peak period of behavioral and cognitive vulnerability to general anesthetics in rodents occurs in early postnatal life.<sup>9–11</sup> Based on these studies, the U.S. Food and Drug Administration issued a warning that

Part of the work presented in this article has been presented as a poster at the Sixth Pediatric Anesthesia and NeuroDevelopment Assessment Symposium in New York, New York, April 14, 2018, and as a poster at the Forty Eighth Society for Neuroscience Annual Meeting in San Diego, California, November 4, 2018.

Submitted for publication December 3, 2018. Accepted for publication June 24, 2019. From the Department of Anesthesiology and Critical Care Medicine, Johns Hopkins School of Medicine, Baltimore, Maryland.

Copyright © 2019, the American Society of Anesthesiologists, Inc. All Rights Reserved. *Anesthesiology* 2019; 131:1077–91. DOI: 10.1097/ALN.0000000000002904

lengthy or repeated exposure to general anesthetics and sedative drugs from the third trimester of prenatal development through the first 3 yr of life may cause lasting impairment in the cognitive function.<sup>12</sup> The molecular and cellular mechanisms underlying this phenomenon remain poorly understood.

Most studies investigating anesthetic neurotoxicity have focused on neuronal development.<sup>7,13</sup> However, brain function is also dependent on the myelin-forming oligodendrocytes, which undergo critical developmental events during the putative window of vulnerability. Myelination involves proliferation of oligodendrocyte progenitor cells, differentiation of oligodendrocyte progenitor cells into mature oligodendrocytes, and ensheathment of axons. Myelin is critical for neurotransmission in the central nervous system (CNS), and disruptions of myelin function are associated with neurologic and psychiatric disorders.<sup>14,15</sup> In this study, we test the hypothesis that early postnatal exposure to isoflurane affects oligodendrocyte development and myelin formation in the hippocampus in an *in vivo* mouse model. To establish the extent to which isoflurane-induced deficits can be attributed to impaired myelination, we employed clemastine, an antimuscarinic drug approved for multiple sclerosis therapy, which promotes oligodendrocyte differentiation and myelination and reverses the phenotype of several murine disease models involving demyelination.<sup>16,17</sup>

Exposure to general anesthetics has been shown to impact molecular signaling pathways implicated in the dynamic maintenance of cellular homeostasis and development.<sup>13</sup> Recently, mammalian target of rapamycin (mTOR) signaling has emerged as a critical integrator of activity of nerve cells and synaptic inputs that in turn affect many cellular metabolic processes.<sup>18</sup> Studies have implicated mTOR signaling in neurodevelopmental and neuropsychiatric disorders.<sup>19</sup> We previously showed that isoflurane disrupts development of newborn hippocampal neurons and synaptic formation *via* activation of the mTOR pathway.<sup>7,20</sup> In this study, we further investigate the role of mTOR in isoflurane-induced neurotoxicity in mouse oligodendrocyte development and myelination using mTOR activity markers and rapamycin, a mTOR pathway inhibitor. We explored the effects on axon-oligodendrocyte precursor synapses, which are thought to be critical for turning oligodendrocyte development to match neuronal activity.<sup>21–23</sup> Activity in the mTOR pathway mediates DNA methylation in neurons<sup>24</sup> and cancer cells,<sup>25</sup> and it has been reported that DNA methylation is a well-recognized epigenetic modification that regulates oligodendrocyte development and is necessary for efficient myelin formation.<sup>26–28</sup> Thus, the effect of general anesthetics and mTOR activation on DNA methylation level in oligodendrocytes has also been investigated.

## Materials and Methods

### Animal Paradigm and Experimental Timeline

A total of 120 (61 male and 59 female) immature C57BL/6 mice (body weight =  $4.4 \pm 0.9$  g at postnatal day 7) were used in this study. Eighty-four (44 male and 40 female) of them were randomly selected for the rapamycin experiment and 36 (17 male and 19 female) for the clemastine experiment. Sex was not factored into the research design as a biologic variable. Both sexes were equally represented in all experiments. All study protocols involving mice were approved by the Animal Care and Use Committee at Johns Hopkins University (Baltimore, Maryland) and conducted in accordance with National Institutes of Health (Bethesda, Maryland) guidelines for care and use of animals. Experimental procedures followed the modified protocols from a previously published journal.<sup>7</sup>

At postnatal day 7, animals were exposed to isoflurane or room air for 4 h. From postnatal days 21 to 35, half of the isoflurane-exposed mice were injected intraperitoneally bidaily with rapamycin ( $n = 28$  per group) or fed daily with clemastine through gastric gavage ( $n = 12$  per group). The other half were injected with vehicle of rapamycin or fed with vehicle of clemastine.

For the rapamycin experiment, a subset of mice from each group was euthanized at postnatal day 35 for immunohistochemistry ( $n = 8$  per group) or Western blotting ( $n = 8$  per group). The remaining mice underwent behavioral testing for spatial learning and memory functions between postnatal days 56 and 62 ( $n = 12$  for each group). After behavior tests, two mice from each group were processed for electron microscopy at postnatal day 63. Only behavior tests were conducted for the clemastine feeding experiment ( $n = 12$  for each group; fig. 1A).

### Isoflurane Exposure

At postnatal day 7, two thirds of the mice were evenly distributed across littermate groups and were randomly selected for isoflurane exposure. The other one third of the mice stayed in room air as a naive control. Volatile anesthesia exposure was accomplished using a Supera (USA) tabletop portable nonrebreathing anesthesia machine. Three percent isoflurane mixed in 100% oxygen was initially delivered in a closed chamber for 3 to 5 min, and after loss of righting reflex, animals were transferred to the specially designed plastic tubes. A heating pad ( $36.5^\circ\text{C}$ ) was placed underneath the exposure setup. The mice were exposed to 1.5% isoflurane carried in 100% oxygen for 4 h. A calibrated flowmeter was used to deliver oxygen at a flow rate of 5 l/min, and an agent-specific vaporizer was used to deliver isoflurane. During isoflurane exposure, mice were monitored for change in physiologic state using the noninvasive MouseOx plus instrument (STARR Life Sciences, USA). A collar clip connected to the instrument was placed on the neck and

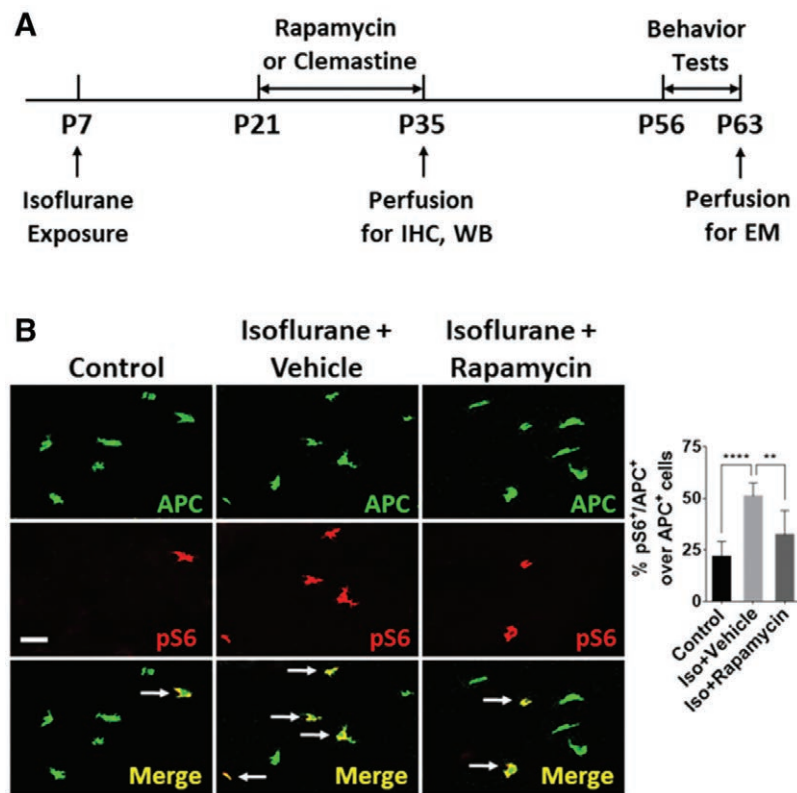


**Fig. 1.** (A) Experimental timeline. A total of 120 mice (84 for rapamycin injection and 36 for clemastine feeding experiments) were used in this study. At postnatal day 7, two thirds of the mice were exposed to isoflurane (Iso) carried for 4 h, and the other one third of the animals remained in room air as naive controls. From postnatal days 21 to 35, isoflurane-exposed mice were injected intraperitoneally with rapamycin or vehicle at 48 h intervals, or daily fed with clemastine or vehicle. Mice were euthanized at postnatal day 35 for immunohistochemistry and Western blotting, or at postnatal day 63 for electron microscopy. The novel objective position recognition test and Y-maze test were performed during postnatal days 57 to 62. (B) Effect of early isoflurane exposure on mammalian target of rapamycin pathway activity in oligodendrocytes of hippocampus fimbria. Coronal brain sections from control, isoflurane exposure, and isoflurane plus rapamycin groups were immunostained with adenomatous polyposis coli (APC; green) and phospho-S6 (pS6; red) antibodies. Arrows indicate phospho-S6-positive and adenomatous polyposis coli-positive double-labeled cells (yellow) in merged images. Scale bar = 10  $\mu$ m. The histogram shows quantitative results. In isoflurane-exposed mice, the ratio of phospho-S6-positive/adenomatous polyposis coli-positive over adenomatous polyposis coli-positive cells is dramatically increased compared to control, and this increase is reversed with rapamycin treatment.  $n = 8$  for each group; one-way ANOVA; \*\* $P < 0.01$ ; \*\*\*\* $P < 0.0001$ . Error bars: SD. EM, electron microscopy; IHC, immunohistochemistry; WB, western blot.

a temperature probe placed on the skin of the abdomen. Ten-minute readings with 1-h intervals were taken. Data were collected at four time-points and averaged for each case. The skin temperature ( $34.1 \pm 0.8^\circ\text{C}$ ), pulse distention ( $168.9 \pm 36.6 \mu\text{m}$ ), heart rate ( $376.8 \pm 94.1$  beats/min), breath rate ( $77.4 \pm 35.8$  breaths/min), and oxygen saturation ( $99.3 \pm 0.3\%$ ) were recorded. After the isoflurane exposure, mice were returned to their mothers together with their littermates upon regaining righting reflex. All animals (100%) survived the isoflurane exposure.<sup>7</sup>

### Rapamycin Injection

A total of 84 mice were equally divided into three groups: (1) naive control, (2) isoflurane exposure plus vehicle, and (3) isoflurane plus rapamycin injection. From postnatal days 21

to 35, half of the isoflurane-exposed mice (group 3;  $n = 28$  per group) were injected intraperitoneally with 0.2% rapamycin dissolved in vehicle solution and the other half with vehicle only (group 2;  $n = 28$  per group). Vehicle consisted of 5% Tween 80 (Sigma-Aldrich, USA), 10% polyethylene glycol 400 (Sigma-Aldrich), and 8% ethanol in saline. Mice received 100  $\mu$ l rapamycin or vehicle for each injection at 48-h intervals from postnatal days 21 to 35.<sup>7</sup>

### Clemastine Feeding

In this experiment, 36 animals were also equally divided into three groups as above. Clemastine (Tocris Bioscience, United Kingdom) was dissolved in dimethylsulfoxide (Sigma-Aldrich) at 10 mg/ml followed by further dilution in double distilled water into 1 mg/ml. From postnatal days

21 to 35, half of the isoflurane exposed mice ( $n = 12$  for each group) were fed clemastine (10 mg/kg) daily *via* gastric gavage using plastic feeding tubes (gauge 22; Instech, USA), and the other half ( $n = 12$  for each group) were fed same volume of 10% dimethylsulfoxide as vehicle.<sup>16,17</sup>

### Behavior Tests

The novel object position recognition test and Y-maze test were performed at the last week of the survival period (postnatal days 56 to 62).<sup>7</sup> Experimenters were blinded to condition when behavioral tests were carried out and quantified.

1. Novel object position recognition test: The test was assessed in a 27.5 cm × 27.5 cm × 25 cm opaque chamber. During the pretest day (day 1), each mouse was habituated to the chamber and allowed to explore two identical objects (glass bottles, 2.7 cm diameter, 12 cm height, and colored paper inside) for 15 min. The mouse was then returned to its home cage for a retention period of 24 h. On the test day (day 2), the mouse was reintroduced to the chamber and presented with one object that stayed in the same position (old position) while the other object was moved to a new position (novel position). A 5-min period of movement and interaction with the objects was recorded with a video camera that was mounted above the chamber, and exploratory behavior was measured by a blinded observer. Exploratory behavior was defined as touching the object with snouts. The numbers of exploratory contacts with the novel object and with the old object were respectively recorded, and the ratios over the total exploratory contact numbers were calculated.
2. Y-maze test: In the pretest phase (day 1), mice explored and habituated in the start arm (no visual cue) and one out of two possible choice arms with overt visual cue (old arm) for 15 min. This was followed by the recognition phase (day 2) 24 h later, in which the animals could move freely in the three arms and choose between the two choice arms (old arm and novel arm) after being released from the start arm. The timed trials (5 min) were video recorded as well as graded by an observer blinded to the conditions for exploration time in each choice arm, and the percentages over total exploratory time were calculated.

### Immunohistochemistry

During postnatal days 30 to 35, 5-bromo-2'-deoxyuridine (Abcam, United Kingdom) was injected intraperitoneally at 50 mg/kg daily in animals randomly selected from three groups ( $n = 8$  for each group). At postnatal day 35, mice were perfused with 40 ml 4% paraformaldehyde in phosphate buffered saline. Brains were removed and postfixed at 4°C overnight, followed by 30% sucrose in phosphate buffered saline at 4°C for 48 h. The brains were coronally sectioned in 40- $\mu$ m thickness using a freezing microtome. For each brain, 72 sections containing fimbria were collected

in a 24-well tissue culture plate, and they were divided into 12 wells in a rotating order (six sections per well). Seven wells of sections were immunostained for (1) phospho-S6 and adenomatous polyposis coli, (2) 5-bromo-2'-deoxyuridine and neural/glial antigen 2, (3) adenomatous polyposis coli and platelet-derived growth factor receptor alpha, (4) vesicular glutamate transporter 1 and neural/glial antigen 2, (5) myelin basic protein, (6) DNA methyltransferase 1 and Olig2 (oligodendrocyte transcription factor marker), and (7) 5-methylcytosine and adenomatous polyposis coli. For 5-bromo-2'-deoxyuridine staining, sections were pretreated with 2 Normal HCl to denature DNA (37°C; 45 min), and with 2 × 15 min borate buffer (pH 8.5) to neutralize the HCl. After 3 × 10 min phosphate buffered saline washing, sections were blocked in 10% normal goat serum and 0.1% Triton X-100 (Sigma-Aldrich) for 60 min, followed by primary antibody incubation at 4°C overnight. Primary antibodies used in this study were rabbit anti-phospho-S6 (1:1,000; Cell Signaling, USA), mouse anti-5-bromo-2'-deoxyuridine (1:200; Abcam), rabbit anti-neural/glial antigen 2 (1:200; Millipore, USA), mouse anti-adenomatous polyposis coli (1:2,000; Millipore), mouse anti-myelin basic protein (1:500; Santa Cruz Biotechnology, USA), rabbit anti-platelet-derived growth factor receptor alpha (1:500; Lifespan Bio, USA), mouse anti-vesicular glutamate transporter 1 (1:200; Abcam), mouse anti-DNA methyltransferase 1 (1:100; Santa Cruz Biotechnology), rabbit anti-Olig2 (1:2,000; Abcam), and rabbit anti-5-methylcytosine (1:2,500; Abcam). After 3 × 10-min washes in phosphate buffered saline, sections were incubated with secondary antibodies for 2 h: Alexa 488-conjugated goat anti-rabbit IgG (1:300; Invitrogen, USA) mixed with Cy3-conjugated goat anti-mouse IgG (1:600; Jackson ImmunoResearch Labs, USA), or Alexa 488-goat anti-mouse IgG (1:300; Invitrogen) mixed with Cy3-conjugated goat anti-rabbit IgG (1:600; Jackson ImmunoResearch Labs). After 3 × 10-min phosphate buffered saline washes, sections were mounted onto slides, air-dried, and cover-slipped.<sup>21</sup>

### Cell Counting and Immunofluorescence Intensity Analysis in Fimbria

The sections were observed and imaged using a Leica 4000 confocal microscope (Germany). All single- or double-immunolabeled cells within hippocampal fimbria area were counted using ImageJ with cell counter plugin (National Institutes of Health). The criteria for counting mTOR active oligodendrocytes required a cell to have both phospho-S6-positive (in red channel) and adenomatous polyposis coli-positive (in green channel) cytoplasm, and a merged image of double-labeled cells appeared yellow (fig. 1B). Proliferating oligodendrocyte progenitor cells and 5-methylcytosine-positive oligodendrocytes were counted for cells that have 5-bromo-2'-deoxyuridine-positive or 5-methylcytosine positive nuclei and neural/glial antigen 2-positive or adenomatous polyposis coli-positive cytoplasm.

However, both DNA methyltransferase 1 and Olig2 reactivity were seen in nuclei. Identification of excitatory axon–oligodendrocyte progenitor cell synapses involved vesicular glutamate transporter 1–positive terminal boutons closely apposing on the surface of neural/glial antigen 2–positive oligodendrocyte progenitor cells. For adenomatous polyposis coli and platelet-derived growth factor receptor alpha double-stained sections, almost no double-labeled cells were seen, which means these two markers label cells in different oligodendrocyte development stages without overlapping.

Images containing fimbria were taken at 20× magnification in red (Cy3), green (Alexa 488), and merged channels. All single- (Cy3<sup>+</sup> or Alexa 488<sup>+</sup>) and double-labeled cells in fimbria were counted. Images were opened and initialized in ImageJ. The fimbria area was outlined using the “Freehand” tool. “Plugins,” “Analysis,” and “Cell Counter” tools were selected, and each labeled cell inside was clicked, with which each counted cell was marked, preventing the same cell from being counted twice. The numbers of counted cells were automatically recorded. The ratio of a specific marker labeled oligodendrocytes (such as yellow-colored phospho-S6–positive/ adenomatous polyposis coli–positive cells over all green adenomatous polyposis coli–positive cells in fig. 1B) was calculated. For each case, numbers from 12 fimbria images (six sections, both sides) were averaged. There was almost no double-staining for adenomatous polyposis coli and platelet-derived growth factor receptor alpha. We then used the ratio of adenomatous polyposis coli–positive over platelet-derived growth factor receptor alpha–positive cells to evaluate the maturation of oligodendrocyte lineage cells. For axon–oligodendrocyte progenitor cells synapse, five neural/glial antigen 2–positive cells from each image (60 cells for each case) were randomly selected, and photos were taken in a higher magnification (40×). All vesicular glutamate transporter 1–positive terminal boutons apposing on each selected cell were counted with ImageJ, and average numbers were calculated.

The fluorescence intensity of myelin basic protein immunoreactivity in fimbria was also quantitatively analyzed using ImageJ. Photos of the fimbria area from immunostained sections were taken at 20× magnification. Identical photo exposure was set for all groups. The image was opened with ImageJ, and an outline of fimbria was drawn with “Freehand” tool. The “set measurements” was selected from the analyze menu, and “integrated density” was activated. A region in lateral ventricle was selected as background. The final myelin basic protein intensity of fimbria area equals measured density minus background.

### Western Blotting

Eight animals from each group were quickly perfused with cold saline on day 35. From the medial aspect of the hemisphere, the hippocampus was exposed and separated from brain tissue. Fimbria located in the ventrolateral side of the

hippocampus were easily identified by their bright white color under dissection microscope, and then removed with fine forceps. Fimbria tissue was lysed in the lysis buffer, homogenized with a bullet bender (Next Advance, USA), and centrifuged. The supernatant was taken and stored in –80°C. The next day, samples were prepared with 1:1 denaturing sample buffer (Bio-Rad, USA), boiled for 5 min, and run on 4 to 12% Bis-Tris Protein Gels (Invitrogen) in running buffer (Invitrogen) with 150 volts for about 1 h. The proteins were transferred to nitrocellulose blotting membranes (Invitrogen). Blots were probed with anti-neural/glial antigen 2 (1:200; Millipore), anti-NK2 homeobox 2 (1:200; Abcam), anti-myelin basic protein (1:500; Santa Cruz Biotechnology), anti-DNA methyltransferase 1 (1:100; Santa Cruz Biotechnology), and anti-β-actin antibodies (1:1,000; Cell Signaling Technology). The membranes with the primary antibodies were stored in 4°C overnight. After incubation in secondary antibodies (1:2,000; Cell Signaling Technology) for 1 h, blots were visualized using an ECL Western blotting substrate kit (Pierce Biotechnology, USA). Images were acquired using the ChemiDoc imaging system (Bio-Rad) and were quantitated with ImageJ. First, the images were opened using “File>Open.” The rectangles around all lanes (each lane includes bands for detected marker and β-actin) were drawn by choosing “Rectangular Selection.” Then, proceeding to “Analyze>Gels>Plot Lanes,” peaks were generated representing the density of bands, followed by clicking the “Straight Line” tool to enclose the peaks and selecting the “Wand” tool to highlight the peaks. After this, “Analyze>Gels>Label Peaks” was used to get numbers for the peak area (band intensity). The ratios of band density of oligodendrocyte lineage markers over β-actin were calculated.<sup>21</sup>

### Electron Microscopy

Two animals from each group were perfused with 2% glutaraldehyde (Electron Microscopy Sciences, USA) plus 2% paraformaldehyde (Electron Microscopy Sciences) in phosphate buffered saline at postnatal day 63 (after behavior tests) and postfixed at 4°C for 1 week. Brains containing fimbria were dissected into small blocks (2 mm × 2 mm × 2 mm). The blocks were placed into 1% osmium tetroxide (Electron Microscopy Sciences) for 1 h, stained in 0.5% uranyl acetate (Electron Microscopy Sciences) overnight, and dehydrated in a series of alcohols followed by propylene oxide for 3 h. After being infiltrated with a 1:1 mixture of propylene oxide and EMBED-812 embedding resin (Electron Microscopy Sciences) for 3 h, the blocks were embedded with the same resin in the plastic templates at 60°C overnight.<sup>21</sup> Parasagittal semithin sections (1 μm) were cut and stained with 1% Toluidine blue (Sigma-Aldrich) for preliminary light microscopy observation. Then, 90-nm ultrathin sections were cut, picked up on Forvar-coated slotted grids (Electron Microscopy Sciences), and stained with 0.5% uranyl acetate and 0.5% lead citrate (Electron

Microscopy Sciences). Thin sections were observed and imaged with a Hitachi 7600 transmission electron microscope (Chiyoda, Japan). For each case, 10 photos were randomly photographed at 20,000 $\times$ . The thickness of myelin was quantitatively measured by determining the g-ratio, which was calculated by dividing the diameter of the axon by the diameter of the entire myelinated fiber as previously described. ImageJ was used by first opening ultrastructural images. The scale was set according to the scale bar in the images by selecting "Analyze>Set Scale." The "straight line tool" was selected to measure axonal caliber and diameter of myelinated axons. One hundred axons per group (2 animals, 50 from each) were randomly selected and quantitatively analyzed ( $n = 100$ ).<sup>16</sup>

### Statistical Analysis

The statistics were performed with GraphPad Prism 6 (USA) program. The sample size was based on our previous experience with this design. No *a priori* statistical power calculation was conducted. Normal distribution was verified using the D'Agostino–Pearson test. Data for immunohistochemistry, Western blotting, and electron microscopy were analyzed using one-way ANOVA. The factor of variable was comparisons among groups (control *vs.* isoflurane plus vehicle *vs.* isoflurane plus rapamycin). The behavior tests were analyzed with two-way ANOVA. For this analysis, the second factor was the animal's choice between old *versus* novel positions (or arms), and only the values for this variable in each individual group were compared. The Tukey *post hoc* test was employed for intergroup comparisons. The two-tailed test was set according to convention. The criterion for significant difference was set *a priori* at  $P < 0.05$ . In this study, all results were expressed as mean  $\pm$  SD. The sample size "n" represents the number of animals for each group. The only exception is g-ratio analysis with electron microscopy, in which "n" indicates the number of randomly selected axons from two mice per group ( $n = 100$ ). This analysis method is extensively applied for g-ratio study.<sup>16</sup> Because all animals survived tests, there were no missing data in this study. No exclusions for outliers were made in this study. In some experiments, the sample size was increased in response to peer review.

## Results

### Effect of Early Isoflurane Exposure on mTOR Activity in Oligodendrocytes in Hippocampal Fimbria

All experiments compared the three groups as follows: naive control, isoflurane exposure plus vehicle, and isoflurane exposure plus treatment (rapamycin or clemastine). We first assayed for activity in the mTOR pathway in oligodendrocytes by double-labeling for phospho-S6, a reliable reporter of activity in this pathway,<sup>29</sup> and adenomatous polyposis coli, a standard marker for oligodendrocyte. In the control group, 22  $\pm$  7% adenomatous polyposis coli–positive

oligodendrocytes in fimbria were also immunolabeled for phospho-S6. There was a profound increase in the percentage of phospho-S6–positive/ adenomatous polyposis coli–positive cells over adenomatous polyposis coli–positive cells to 51  $\pm$  6% in isoflurane exposure mice ( $P < 0.0001$ ). However, this increase of phospho-S6–positive/adenomatous polyposis coli–positive cells over adenomatous polyposis coli–positive cells was prevented by treatment with rapamycin (32  $\pm$  12%;  $P = 0.001$ ). These data indicate early exposure of a general anesthetic agent causing a lasting increase in the activity of the mTOR signaling pathway in the oligodendrocytes of hippocampus white matter, and rapamycin attenuates this increase.

### Effect of Isoflurane Exposure on Spatial Learning

Next, we asked whether isoflurane exposure impairs spatial learning and memory behaviors using the novel objective position recognition test (fig. 2A) and Y-maze test (fig. 2B), and whether treatment with rapamycin or clemastine restores these functions in our exposure paradigm.

1. Rapamycin study: In the novel object position recognition test, control animals made 58  $\pm$  8% contacts with the object that had been repositioned as compared to 42  $\pm$  8% contacts with the unchanged object ( $P < 0.0001$ ). The isoflurane-exposed mice made essentially equal contacts at both objects (53  $\pm$  6% *vs.* 47  $\pm$  6% times;  $P = 0.398$ ). Rapamycin treatment restored the performance to near control levels (55  $\pm$  8% *vs.* 45  $\pm$  8% times;  $P = 0.016$ ; fig. 2C). In the Y-maze test, control animals exhibited a higher percentage of exploration time in novel arm (58  $\pm$  5% exploration time) compared to the old one (42  $\pm$  5% exploration time;  $P < 0.0001$ ). Isoflurane-exposed animals without rapamycin treatment had equal exploration times in both arms (50  $\pm$  5% *vs.* 50  $\pm$  5% duration;  $P = 0.999$ ), and rapamycin treatment restored performance in this task (56  $\pm$  8% *vs.* 44  $\pm$  8% duration;  $P < 0.001$ ; fig. 2D).
2. Clemastine study: In the novel object recognition test, control animals made more contacts with the object in the novel position (57  $\pm$  8% *vs.* 43  $\pm$  8% times;  $P = 0.007$ ), but isoflurane exposed animals exhibited no exploration preference (51  $\pm$  10% *vs.* 49  $\pm$  10% times;  $P = 0.998$ ). Clemastine treatment increased the difference near the control cases (56  $\pm$  7% *vs.* 44  $\pm$  7% times;  $P = 0.028$ ; fig. 2E). Similarly, in the Y-maze test, unlike controls (58  $\pm$  6% *vs.* 42  $\pm$  6% duration;  $P < 0.0001$ ), isoflurane-exposed mice spent identical time in both old and novel arms (51  $\pm$  7% *vs.* 49  $\pm$  7% duration;  $P = 0.999$ ), and this effect of isoflurane was reversed by clemastine treatment (57  $\pm$  6% *vs.* 43  $\pm$  6% duration;  $P < 0.001$ ; fig. 2F).

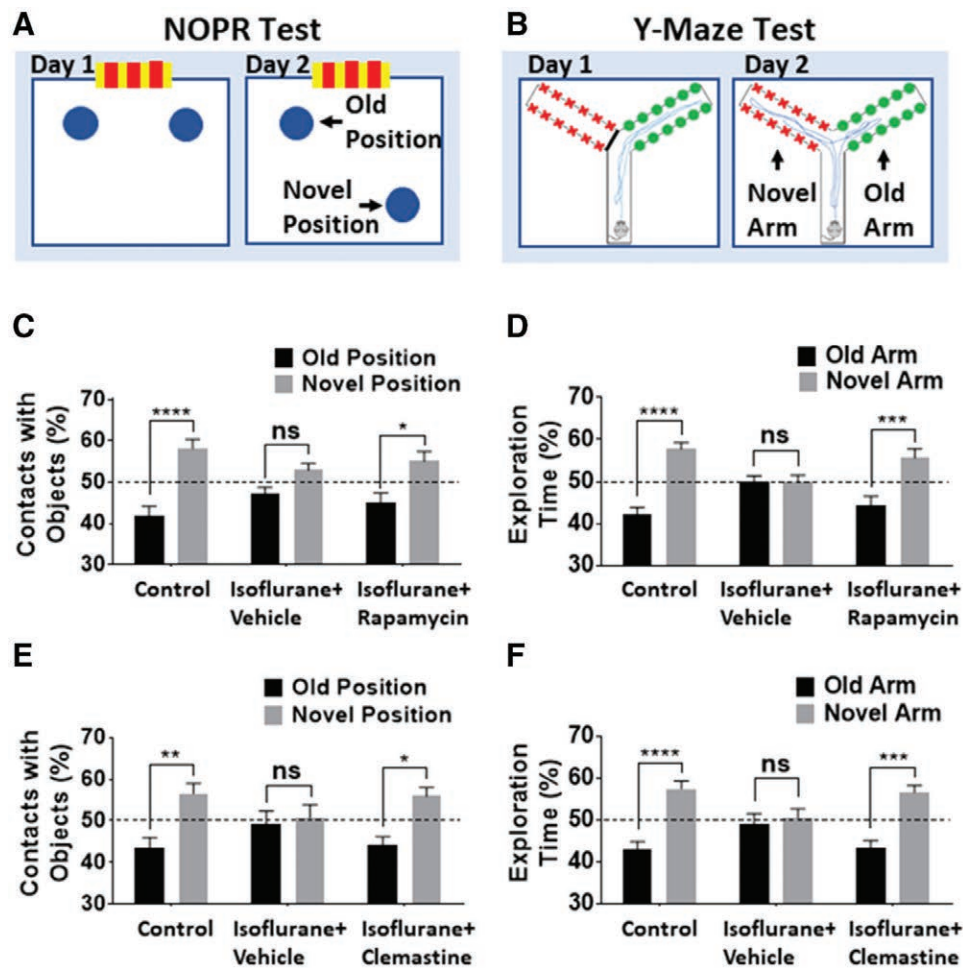


**Fig. 2.** Isoflurane impairs cognitive functions *via* mammalian target of rapamycin activity. (A) Novel object recognition test (NOPR). On day 1, mice were allowed to explore two identical objects in an opaque chamber. On day 2, one object was moved to a novel position. Exploratory behavior was defined as the number of object-contacting with snouts. (B) Y-maze test. On day 1, mice habituated in the start arm and one choice arm. On day 2, the animal could choose between two arms. Exploration time in both arms was respectively recorded. (C) Novel object recognition test for rapamycin study. Control animals made more contact with the object in the novel position than that in the old position. Isoflurane-exposed mice have identical contacts for both positions. Rapamycin treatment restores performance to near control levels. (D) Y-maze study. Control animals stayed in the novel arm for longer time than in the old arm. Isoflurane-exposed animals stayed in both arms for same time. Rapamycin treatment reversed this ratio to near control. (E) Novel object recognition test for clemastine study. Control animals spent more time exploring the object in the novel position, but isoﬂurane-exposed animals exhibited no exploration preference. Clemastine treatment increased difference near the level of control animals. (F) Y-maze test. Similarly, isoﬂurane mice spent identical time for both arms, but this effect of isoﬂurane was reversed by feeding clemastine. The statistics were two-way ANOVA.  $n = 12$  for each group; \* $P < 0.05$ ; \*\* $P < 0.01$ ; \*\*\* $P < 0.001$ ; \*\*\*\* $P < 0.0001$ ; ns, no signiﬁcance. Error bars: SD.

### Effects of Isoflurane on Oligodendrocyte Development

In order to measure the proliferation of oligodendrocyte progenitor cells, the brain tissue was immunolabeled with antibodies against 5-bromo-2'-deoxyuridine and an oligodendrocyte progenitor cells marker, neural/glial antigen 2. We examined proliferating oligodendrocyte progenitor cells by counting 5-bromo-2'-deoxyuridine and neural/glial antigen 2 double-labeled cells in fimbria. We counted  $49 \pm 14\%$  neural/glial antigen 2-positive oligodendrocyte

progenitor cells in controls, and  $27 \pm 9\%$  neural/glial antigen 2-positive cells in isoﬂurane-exposed animals were 5-bromo-2'-deoxyuridine-positive ( $P = 0.001$ ). This ratio number increased to  $47 \pm 7\%$  ( $P = 0.003$ ) in the isoﬂurane plus rapamycin injection group (fig. 3A). Interestingly, we found that neural/glial antigen 2 expression from Western blot in the isoﬂurane exposure group ( $83 \pm 20\%$  intensity over  $\beta$ -actin) is slightly lower than the control ( $87 \pm 15\%$ ;  $P = 0.882$ ) and rapamycin treatment groups ( $89 \pm 17\%$ ;  $P = 0.819$ ), but there is no statistical difference

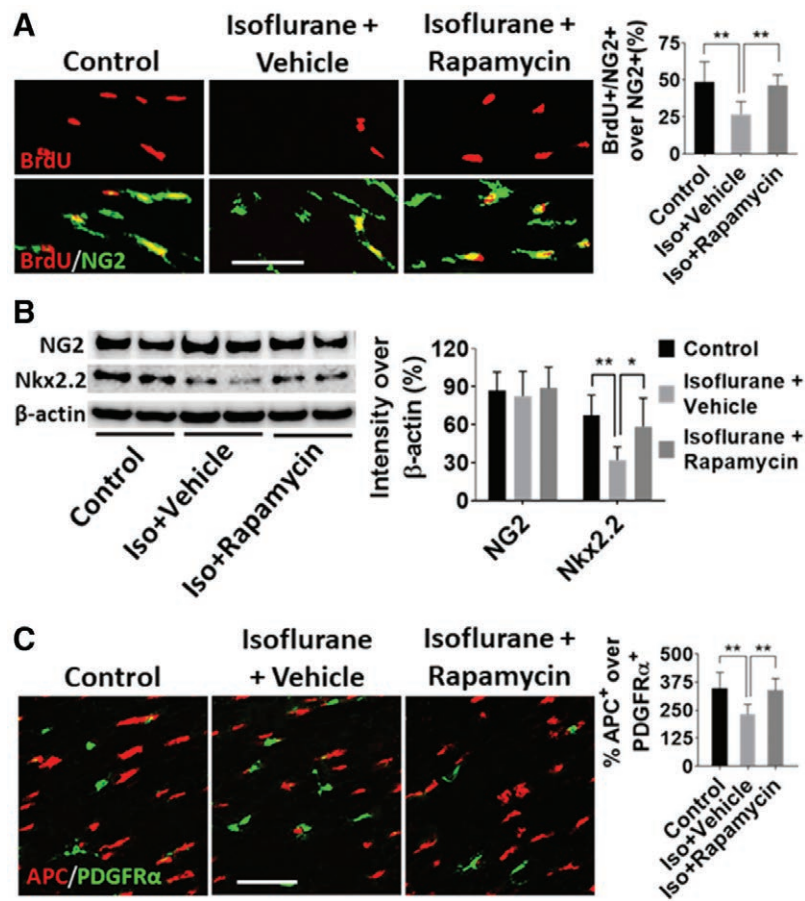


**Fig. 3.** The effect of isoflurane (Iso) exposure and rapamycin treatment on oligodendrocyte development in fimbria. (A) Oligodendrocyte progenitor cell proliferation was detected with 5-bromo-2'-deoxyuridine and neural/glial antigen 2 double-immunolabeling. A reduction in 5-bromo-2'-deoxyuridine-positive/neural/glial antigen 2-positive cells in isoflurane-exposed animals was observed compared to the control. This number was increased in isoflurane plus rapamycin injection group. Scale bar = 20 μm. (B) Western blot data indicated that the neural/glial antigen 2 level was not altered by isoflurane exposure and rapamycin administration. Expression of NK2 homeobox 2, a transcript factor for oligodendrocyte differentiation, was downregulated by isoflurane, and rapamycin treatment attenuated this effect. (C) Oligodendrocyte differentiation was analyzed with lineage tracing using immunohistochemistry. The ratio of adenomatous polyposis coli-positive mature oligodendrocyte number over platelet-derived growth factor receptor alpha-positive oligodendrocyte progenitor cells in isoflurane-exposed mice revealed reduction compared to control, and rapamycin treatment increases the ratio. Scale bar = 20 μm. n = 8 for each group; one-way ANOVA; \*P < 0.05; \*\*P < 0.01; ns, no significance. Error bars: SD. APC, adenomatous polyposis coli; PDGFR-α, platelet-derived growth factor α.

among groups (fig. 3B). However, expression level of NK2 homeobox 2, a transcription factor that identifies oligodendrocyte differentiation, was downregulated by isoflurane ( $67 \pm 16\%$  vs.  $32 \pm 10\%$  intensity over β-actin;  $P = 0.001$ ), and rapamycin attenuated this effect ( $58 \pm 22\%$  intensity over β-actin;  $P = 0.015$ ; fig. 3B). We then performed double-immunolabeling for adenomatous polyposis coli and the oligodendrocyte progenitor cell marker platelet-derived growth factor receptor alpha, and applied oligodendrocyte/oligodendrocyte progenitor cell ratio as a parameter to evaluate the oligodendrocyte differentiation in fimbria.<sup>30</sup> The ratio of the number of adenomatous polyposis coli-positive mature oligodendrocytes over the number of platelet-derived growth factor receptor alpha-labeled

oligodendrocyte progenitor cells in isoflurane-exposed mice ( $233 \pm 43\%$ ) revealed lower than in control ( $347 \pm 70\%$  cells;  $P = 0.002$ ), and rapamycin treatment increases this ratio ( $338 \pm 52\%$  cells;  $P = 0.003$ ; fig. 3C).

To test the effects of isoflurane on axon-oligodendrocyte progenitor cell synapses, we identified excitatory axon-oligodendrocyte progenitor cell synapses in the fimbria as puncta that were immunopositive for vesicular glutamate transporter 1, which were closely apposed on neural/glial antigen 2-positive cell bodies. We found that the number of axon-oligodendrocyte progenitor cell synapses on each oligodendrocyte progenitor cell in isoflurane exposure ( $0.8 \pm 0.6$  vGlut1<sup>+</sup> terminals per oligodendrocyte precursor cell) showed a statistically significant reduction compared to



control ( $2.6 \pm 1.2$  terminals per cell;  $P = 0.001$ ), and rapamycin treatment rescued these synapses ( $2.2 \pm 0.7$  per cell;  $P = 0.008$ ) from isoflurane exposure (fig. 4).

### Effects of Isoflurane Exposure on Myelination

To test for changes in myelination after anesthesia exposure, we measured fluorescence intensity of immunolabeling for the myelin basic protein in fimbria. We found an immunointensity reduction in isoflurane exposure ( $70 \pm 18\%$  intensity over control) compared to control conditions ( $100 \pm 17\%$  control;  $P = 0.006$ ), which were partially restored with rapamycin treatment ( $92 \pm 17\%$  rapamycin treatment;  $P = 0.041$ ; fig. 5A). We then conducted Western blot from fimbria tissue to confirm this finding. The band intensity of myelin basic protein over  $\beta$ -actin showed a statistically significant decrease by isoflurane exposure ( $110 \pm 30\%$  vs.  $60 \pm 19\%$  intensity ratio;  $P = 0.002$ ), and expression of myelin basic protein was restored with rapamycin treatment ( $100 \pm 26\%$  intensity ratio;  $P = 0.013$ ; fig. 5B). For further confirmation, we conducted electron microscopy to test for changes in the thickness of myelin wraps after isoflurane exposure.

The quantitative analysis revealed a statistically significant increase of g-ratio (thinner myelin sheath) in isoflurane-exposed animals than control ( $0.76 \pm 0.06$  vs.  $0.79 \pm 0.06$  g-ratio;  $P < 0.001$ ), and rapamycin treatment reversed this difference ( $0.75 \pm 0.05$  g-ratio;  $P < 0.0001$ ; fig. 5C).

### Effects of Isoflurane Exposure on DNA Methylation in Oligodendrocytes

We asked if early exposure to isoflurane has a lasting effect on DNA methylation levels in oligodendrocytes. We observed that  $60 \pm 15\%$  of Olig2<sup>+</sup> cells (a transcription factor marker for oligodendrocyte lineage cells) in control conditions were double-labeled with DNA methyltransferase 1 in fimbria as compared to only  $42 \pm 12\%$  Olig2<sup>+</sup> cells ( $P = 0.027$ ) in the isoflurane exposure group. Rapamycin treatment after isoflurane exposure increased the ratio of DNA methyltransferase 1<sup>+</sup>/Olig2<sup>+</sup> over Olig2<sup>+</sup> cells ( $62 \pm 11\%$  ratio;  $P = 0.01$ ; fig. 6A). Western blots were conducted which confirmed that DNA methyltransferase 1 expression is reduced with isoflurane treatment ( $25 \pm 8\%$  intensity ratio over  $\beta$ -actin) compared to control ( $58 \pm 21\%$  intensity ratio over  $\beta$ -actin;  $P < 0.001$ ).

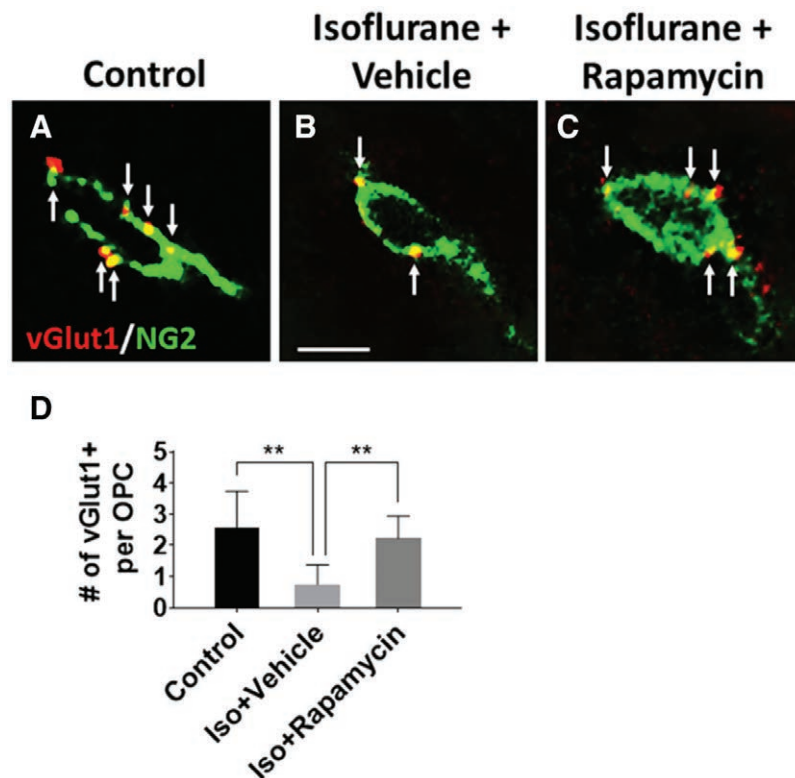


**Fig. 4.** The effect of isoflurane (Iso) exposure and rapamycin treatment on the numbers of excitatory axon–oligodendrocyte progenitor cell (OPC) synapses in fimbria. The vesicular glutamate transporter 1–positive axon–oligodendrocyte progenitor cell synapses were identified with terminals apposing on neural/glial antigen 2–positive oligodendrocyte progenitor cells (arrows indicate these synapses). The number in isoflurane exposure mice was lower than control and rapamycin treatment rescued these axon–oligodendrocyte progenitor cell synapses. Scale bar = 5  $\mu$ m. (A) Control. (B) Isoflurane exposure plus vehicle group. (C) Isoflurane exposure with rapamycin treatment. (D) Graph showing quantitative data.  $n = 8$  for each group; one-way ANOVA; \*\* $P < 0.01$ . Error bars: SD.

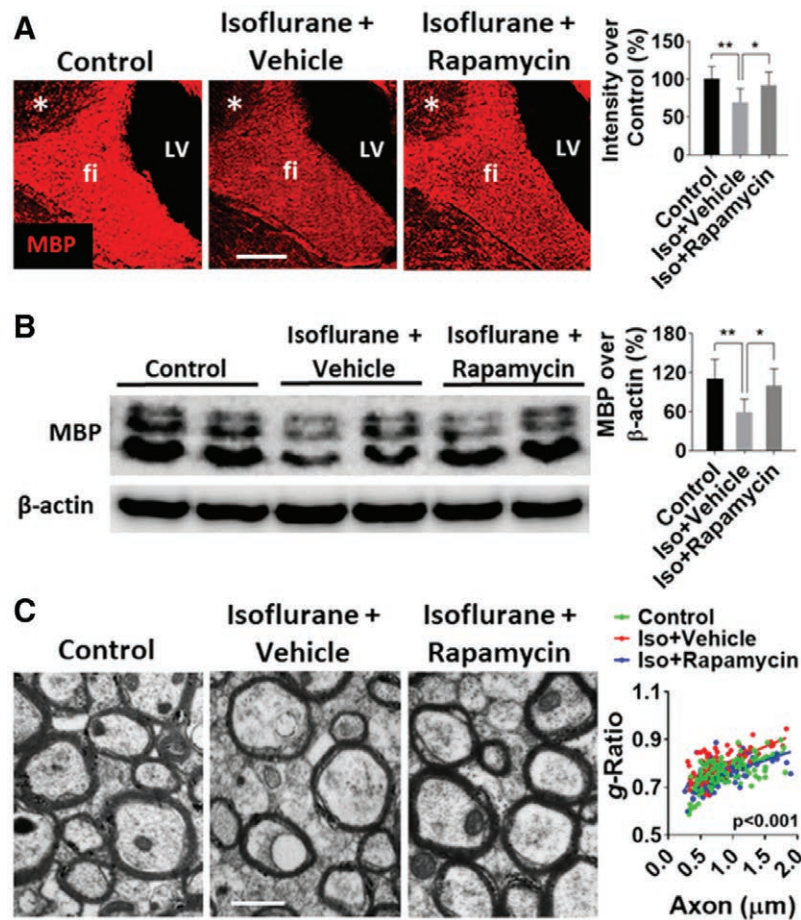


**Fig. 5.** The effect of isoflurane (Iso) exposure and rapamycin treatment on myelination in fimbria. (A) Myelination was quantitatively analyzed with myelin basic protein immunostaining. The myelin basic protein (MBP) intensity in isoflurane-exposed mice was reduced compared to control conditions and is increased with rapamycin treatment. For this analysis, the same exact photo setting was performed for all groups. Asterisk in photos: CA3 of hippocampus; fi: fimbria of hippocampus; LV: lateral ventricle. Scale bar = 200  $\mu$ m. (B) Western blot data indicated expression of myelin basic protein was decreased by isoflurane exposure and then elevated by rapamycin treatment. (C) Electron microscopy analysis was performed in fimbria parasagittal ultrathin sections. The ratio of axonal caliber over diameter of myelinated fiber (g-ratio) was increased in isoflurane-exposed animals (it means decreased myelin thickness) compared to control, and rapamycin treatment reversed this change. Scale bar = 0.5  $\mu$ m. n = 8 for each group in A and B, and n=100 for each group in C. One-way ANOVA; \* $P$  < 0.05; \*\* $P$  < 0.01. Error bars: SD.

and a partial recovery results from rapamycin treatment ( $49 \pm 9\%$  ratio;  $P = 0.006$ ; fig. 6B). In order to determine whether changes in DNA methyltransferase 1 levels have functional significance, we assayed levels of 5-methylcytosine, which is a product of DNA methyltransferase 1-mediated DNA methylation, in oligodendrocytes. Isoflurane exposure decreased the ratio of 5-methylcytosine-positive nuclei over adenomatous polyposis coli-labeled oligodendrocytes ( $33 \pm 13\%$  ratio) relative to control ( $52 \pm 13\%$  ratio;  $P = 0.006$ ), and rapamycin treatment reversed this decrease ( $48 \pm 7\%$  ratio;  $P = 0.031$ ; fig. 6C).

## Discussion

In this study, we report that early postnatal exposure to isoflurane in mice causes a substantial disruption of

oligodendrocyte development and myelination in fimbria of the hippocampus, which is the predominant bundle of efferent axonal fibers from the hippocampus. Proliferation and differentiation of oligodendrocyte progenitor cells are chronically impaired by early isoflurane exposure, as is the formation of synaptic connections between oligodendrocyte progenitor cells and axons. This results in a measurable loss of myelin in the fimbria. Proper connections and communications between hippocampus and the neocortex are critical for performing the cognitive and psychologic functions.<sup>14,31,32</sup> Myelination is essential in establishing connectivity in the growing brain by facilitating rapid and synchronized information transfer across the nervous system. Once thought of as solely a passive insulator, myelin is now understood to be actively involved in the function and

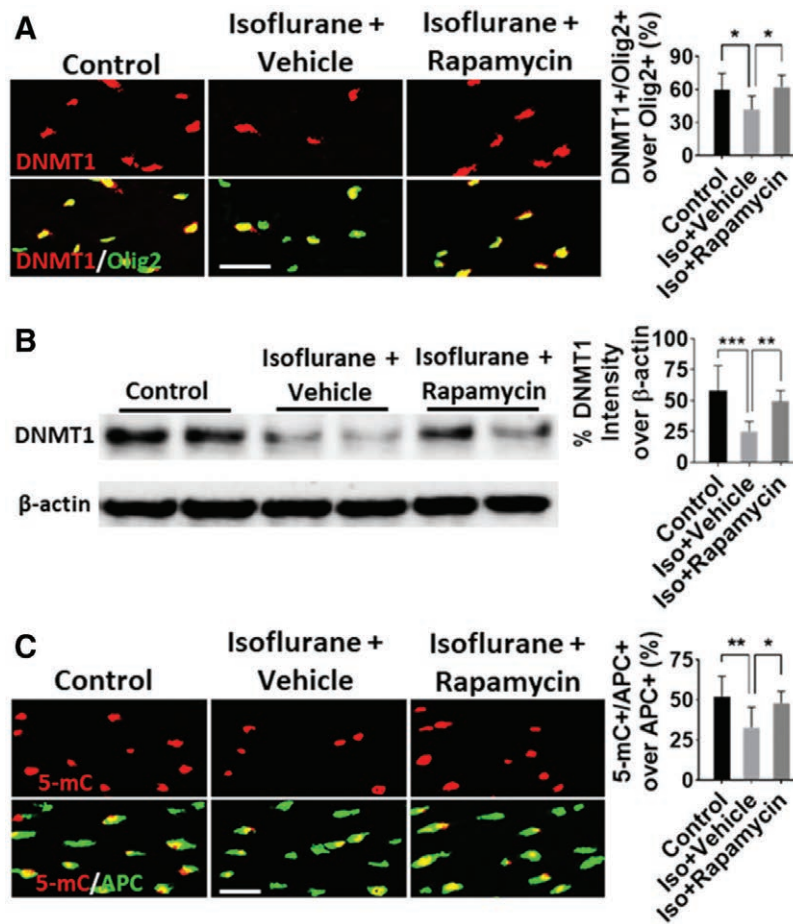


**Fig. 6.** The effect of isoflurane (Iso) exposure and rapamycin treatment on DNA methylation level in oligodendrocytes. (A) DNA methylation level examined with DNA methyltransferase 1 and Olig2 double immunolabeling. The percentage of DNA methyltransferase 1<sup>+</sup>/Olig2<sup>+</sup> over Olig2<sup>+</sup> nuclei in isoflurane-exposed mice was lower than control, and rapamycin increased this ratio. Scale bar = 25  $\mu$ m. (B) Western blot data revealed isoflurane dramatically decreased the DNA methyltransferase 1 level, and rapamycin increased DNA methyltransferase 1. (C) 5-Methylcytosine (5-mC), the product of DNA methylation catalyzed by DNA methyltransferase 1, was detected in nuclei of adenomatous polyposis coli (APC)-positive oligodendrocytes. The ratio of 5-methylcytosine-positive/adenomatous polyposis coli-positive over adenomatous polyposis coli-positive cells showed a statistically significant decrease with isoflurane exposure and rapamycin injection reversed this decrease. Scale bar = 25  $\mu$ m. n = 8 for each group; one-way ANOVA; \* $P$  < 0.05; \*\* $P$  < 0.01; \*\*\* $P$  < 0.001. Error bars: SD.

development of the CNS.<sup>33</sup> Abnormal myelination of axons disrupts the communications between brain regions, and it has been reported that myelin deficits in the hippocampus cause cognitive and psychologic disorders.<sup>34–36</sup> Previous studies have shown an acute increase in apoptosis of oligodendrocytes, the myelin-forming glial cells, with early exposure to isoflurane,<sup>37,38</sup> but our findings demonstrate a lasting effect of anesthesia on oligodendrocyte proliferation and differentiation that results in a decrease in myelination in the hippocampal fimbria.

The process of oligodendrocyte development occurs based on an intrinsic program that is modulated by neurotransmitters and electrical activity in the CNS.<sup>39–41</sup> Axonal terminals release glutamate as a transmitter not only at axonal terminals but also at discrete sites along axons in white

matter.<sup>42</sup> By acting on  $\alpha$ -amino-3-hydroxy-5-methyl-4-isoxazolepropionic acid (AMPA) or *N*-methyl-D-aspartate (NMDA) receptors expressed on oligodendrocyte progenitor cells, glutamate increases the downstream phosphorylation of the cyclic adenosine monophosphate response element-binding protein and release of calcium from intracellular stores,<sup>43</sup> thereby promoting oligodendrocyte progenitor cell proliferation and differentiation. As an agonist of  $\gamma$ -aminobutyric acid type A and glycine receptors,<sup>44</sup> as well as a potential NMDA inhibitor,<sup>45</sup> isoflurane suppresses excitatory neurotransmission.<sup>46</sup> It raises the possibility that a profound direct action on oligodendrocyte progenitor cells, which express both  $\gamma$ -aminobutyric acid and NMDA receptors, is caused by isoflurane during a critical period in development and that this may alter the developmental

program, thus resulting in deficits in myelination. An alternative or complementary explanation may be an indirect effect mediated by the electrochemical synapses that occur between axonal terminals and oligodendrocyte progenitor cells (axon–oligodendrocyte progenitor cell synapses). Formation of glutamatergic axon–oligodendrocyte progenitor cell synapses plays an important role in promoting activity-dependent oligodendrocyte development and maintenance.<sup>21–23</sup> The chronic, lasting effects of isoflurane on neuronal synapses that we have previously shown may translate into reduced activity at axon–oligodendrocyte progenitor cell synapses, thus leading to suppression of oligodendrocyte progenitor cell development. A previous study showed that plasticity of axon–oligodendrocyte progenitor cell synapses is highly dependent on electrical activity.<sup>21</sup> The data in this study further confirm that exposure of isoflurane reduces the number of excitatory (vesicular glutamate transporter 1–positive) axon–oligodendrocyte progenitor cell synapses in hippocampus, which is likely a key mechanism of general anesthetic–induced hypomyelination.

Our previous work has indicated that exposure to isoflurane disrupts the development of hippocampal neurons generated in the early postnatal period by inappropriately increasing activity in the mTOR pathway, and we found that both behavioral and histological changes could be reversed by pharmacologic mTOR inhibition.<sup>7</sup> In the present study, as in neurons, we observe a lasting alteration in the tone of mTOR signaling in oligodendrocytes in the hippocampal fimbria for a protracted period after isoflurane exposure, which appears to be integral to the developmental disruption. We found a substantial improvement in phenotype with rapamycin treatment in this study as well. The mTOR pathway is an intracellular signaling pathway that regulates cellular activities including proliferation, differentiation, apoptosis, metabolism, transmitter release, and other biologic processes.<sup>18</sup> In the past decade, many studies have implicated mTOR signaling in CNS developmental and neuropsychiatric disorders.<sup>19</sup> Two structurally and functionally distinct mTOR-containing complexes have been identified in oligodendrocytes. The first, mTOR complex 1 mTOR, contains the adaptor protein Raptor, which influences myelin basic protein expression *via* an alternative mechanism and is sensitive to the drug rapamycin. The second complex, mTOR complex 2, contains Ritor, and it is thought to control myelin gene expression at the mRNA level and is relatively rapamycin-insensitive.<sup>47</sup>

The mTOR pathway itself plays a complex role in myelination; mTOR activity can either enhance or suppress oligodendrocyte development depending on the context. A study using a mouse line with oligodendrocyte-specific knockdown of mTOR in CNS has provided evidence that mTOR is essential for oligodendrocyte development and myelination.<sup>48</sup> Inhibition of mTOR *via* rapamycin in cultured adult oligodendrocyte progenitor cells or in a mouse model starting at 6 weeks of age results in oligodendrocyte

differentiation deficits along with reduced expression of major myelin proteins and mRNAs.<sup>49–51</sup> In contrast, activation of mTOR induced by tuberous sclerosis complex–1 or –2 gene mutations in early oligodendrocyte progenitor cells caused white matter abnormalities, including myelin deficits in CNS.<sup>52–54</sup> A bidirectional action of the phosphoinositide 3-kinase-protein kinase B–mTOR (PI3K–Akt–mTOR) axis in myelination has also been reported in studies of the peripheral nervous system. If tuberous sclerosis complex–1 deletion occurs in early developmental stages in Schwann cells, mTOR hyperactivity arrests the process by which Schwann cells ensheath axons. If mTOR activity is increased in Schwann cells after they have begun wrapping around axons, there is actually an increase in myelination.<sup>55</sup> Thus, oligodendrocyte development and myelination may be dependent on precise balance and timing in mTOR signaling. Either increasing or decreasing levels of mTOR complex 1 activity interferes with oligodendrocyte differentiation and causes potentially causes hypomyelination.<sup>56</sup>

While we do not yet have a clear picture of how changes in mTOR activity act on oligodendrocytes, our data indicate changes in DNA methylation as a promising direction. Recent work shows developmental anesthetic toxicity may involve epigenetic modulation<sup>57</sup> and that DNA methylation plays an important role in regulating oligodendrocyte progenitor cell proliferation and differentiation.<sup>26–28</sup> Intriguingly, mTOR signaling has been shown to negatively regulate DNA methylation *via* an action on DNA methyltransferase 1,<sup>24,25</sup> suggesting a possible connection between mTOR signaling and oligodendrocyte development. This finding is consistent with our data showing that isoflurane exposure and concomitant increases in mTOR signaling lead to a decrease in DNA methyltransferase 1 expression and DNA methylation in developing oligodendrocytes, and that both of these changes are reversible with rapamycin treatment.

We propose that oligodendrocytes should be further studied both as a potential target in anesthetic neurotoxicity and as a model system in which to further explore the interplay of anesthetics, mTOR signaling, and DNA methylation. Our work is limited by the rodent model, which has well-known confounds related to anesthetic administration in very young, small mice in which physiologic monitoring and control of respiratory function are challenging. In particular, we have chosen to use 100% oxygen as a carrier for isoflurane, which has the beneficial effect of preventing hypoxia in our model system, but which raises the possibility of a combined effect of isoflurane and hyperoxia damage that cannot be fully controlled for in our experimental model. While it is indeed the case that supplemental oxygen is frequently used in pediatric anesthesia practice, it would be ideal to avoid confounds presented by hyperoxia and other physiologic issues *via* studies in large animal models and in cell culture models, and we hope further work in this area will be undertaken in these systems.

## Research Support

This work was funded by grant No. 5R01GM120519 from the National Institutes of Health (Bethesda, Maryland; to Dr. Mintz), and by the Department of Anesthesiology and Critical Care, Johns Hopkins University School of Medicine, Baltimore, Maryland (StAAR award to Dr. Mintz).

## Competing Interests

The authors declare no competing interests.

## Correspondence

Address correspondence to Dr. Mintz: Johns Hopkins University School of Medicine, Department of Anesthesiology and Critical Care Medicine, 720 Rutland Ave., Ross 370, Baltimore, Maryland 21205. [cmintz2@jhmi.edu](mailto:cmintz2@jhmi.edu). Information on purchasing reprints may be found at [www.anesthesiology.org](http://www.anesthesiology.org) or on the masthead page at the beginning of this issue. ANESTHESIOLOGY's articles are made freely accessible to all readers, for personal use only, 6 months from the cover date of the issue.

## References

- Weiser TG, Regenbogen SE, Thompson KD, Haynes AB, Lipsitz SR, Berry WR, Gawande AA: An estimation of the global volume of surgery: A modelling strategy based on available data. *Lancet* 2008; 372:139–44
- Eckenhoff JE: Relationship of anesthesia to postoperative personality changes in children. *AMA Am J Dis Child* 1953; 86:587–91
- Davidson AJ, Disma N, de Graaff JC, Withington DE, Dorris L, Bell G, Stargatt R, Bellinger DC, Schuster T, Arnup SJ, Hardy P, Hunt RW, Takagi MJ, Giribaldi G, Hartmann PL, Salvo I, Morton NS, von Ungern Sternberg BS, Locatelli BG, Wilton N, Lynn A, Thomas JJ, Polaner D, Bagshaw O, Szmuk P, Absalom AR, Frawley G, Berde C, Ormond GD, Marmor J, McCann ME; GAS consortium: Neurodevelopmental outcome at 2 years of age after general anaesthesia and awake-regional anaesthesia in infancy (GAS): An international multicentre, randomised controlled trial. *Lancet* 2016; 387:239–50
- Sun LS, Li G, Miller TL, Salorio C, Byrne MW, Bellinger DC, Ing C, Park R, Radcliffe J, Hays SR, DiMaggio CJ, Cooper TJ, Rauh V, Maxwell LG, Youn A, McGowan FX: Association between a single general anesthesia exposure before age 36 months and neurocognitive outcomes in later childhood. *JAMA* 2016; 315:2312–20
- Coleman K, Robertson ND, Dissen GA, Neuringer MD, Martin LD, Cuzon Carlson VC, Kroenke C, Fair D, Brambrink AM: Isoflurane anesthesia has long-term consequences on motor and behavioral development in infant rhesus macaques. *ANESTHESIOLOGY* 2017; 126:74–84
- Alvarado MC, Murphy KL, Baxter MG: Visual recognition memory is impaired in rhesus monkeys repeatedly exposed to sevoflurane in infancy. *Br J Anaesth* 2017; 119:517–23
- Kang E, Jiang D, Ryu YK, Lim S, Kwak M, Gray CD, Xu M, Choi JH, Junn S, Kim J, Xu J, Schaefer M, Johns RA, Song H, Ming GL, Mintz CD: Early postnatal exposure to isoflurane causes cognitive deficits and disrupts development of newborn hippocampal neurons via activation of the mTOR pathway. *PLoS Biol* 2017; 15:e2001246
- Shen X, Liu Y, Xu S, Zhao Q, Guo X, Shen R, Wang F: Early life exposure to sevoflurane impairs adulthood spatial memory in the rat. *Neurotoxicology* 2013; 39:45–56
- Stratmann G, Sall JW, May LD, Bell JS, Magnusson KR, Rau V, Visrodia KH, Alvi RS, Ku B, Lee MT, Dai R: Isoflurane differentially affects neurogenesis and long-term neurocognitive function in 60-day-old and 7-day-old rats. *ANESTHESIOLOGY* 2009; 110:834–48
- Pontén E, Fredriksson A, Gordh T, Eriksson P, Viberg H: Neonatal exposure to propofol affects BDNF but not CaMKII, GAP-43, synaptophysin and tau in the neonatal brain and causes an altered behavioural response to diazepam in the adult mouse brain. *Behav Brain Res* 2011; 223:75–80
- Zhu C, Gao J, Karlsson N, Li Q, Zhang Y, Huang Z, Li H, Kuhn HG, Blomgren K: Isoflurane anesthesia induced persistent, progressive memory impairment, caused a loss of neural stem cells, and reduced neurogenesis in young, but not adult, rodents. *J Cereb Blood Flow Metab* 2010; 30:1017–30
- Center for Drug Evaluation and Research: Drug safety and availability – FDA drug safety communication: FDA review results in new warnings about using general anesthetics and sedation drugs in young children and pregnant women. U.S. Food and Drug Administration. Available at: <https://www.fda.gov/Drugs/DrugSafety/ucm532356.htm>. Accessed July 19, 2019.
- Vutskits L, Xie Z: Lasting impact of general anaesthesia on the brain: Mechanisms and relevance. *Nat Rev Neurosci* 2016; 17:705–17
- Nickel M, Gu C: Regulation of central nervous system myelination in higher brain functions. *Neural Plast* 2018; 2018:6436453
- Chiaravallotti ND, DeLuca J: Cognitive impairment in multiple sclerosis. *Lancet Neurol* 2008; 7:1139–51
- Liu J, Dupree JL, Gacias M, Frawley R, Sikder T, Naik P, Casaccia P: Clemastine enhances myelination in the prefrontal cortex and rescues behavioral changes in socially isolated mice. *J Neurosci* 2016; 36:957–62
- Li Z, He Y, Fan S, Sun B: Clemastine rescues behavioral changes and enhances remyelination in the cuprizone

- mouse model of demyelination. *Neurosci Bull* 2015; 31:617–25
18. Laplante M, Sabatini DM: mTOR signaling in growth control and disease. *Cell* 2012; 149:274–93
  19. Costa-Mattioli M, Monteggia LM: mTOR complexes in neurodevelopmental and neuropsychiatric disorders. *Nat Neurosci* 2013; 16:1537–43
  20. Xu J, Mathena RP, Xu M, Wang Y, Chang C, Fang Y, Zhang P, Mintz CD: Early developmental exposure to general anesthetic agents in primary neuron culture disrupts synapse formation via actions on the mTOR pathway. *Int J Mol Sci* 2018; 19: 2183
  21. Li Q, Houdayer T, Liu S, Belegu V: Induced neural activity promotes an oligodendroglia regenerative response in the injured spinal cord and improves motor function after spinal cord injury. *J Neurotrauma* 2017; 34:3351–61
  22. Bergles DE, Richardson WD: Oligodendrocyte development and plasticity. *Cold Spring Harb Perspect Biol* 2015; 8:a020453
  23. Gautier HO, Evans KA, Volbracht K, James R, Sitnikov S, Lundgaard I, James F, Lao-Peregrin C, Reynolds R, Franklin RJ, Káradóttir RT: Neuronal activity regulates remyelination via glutamate signalling to oligodendrocyte progenitors. *Nat Commun* 2015; 6:8518
  24. Zhang X, He X, Li Q, Kong X, Ou Z, Zhang L, Gong Z, Long D, Li J, Zhang M, Ji W, Zhang W, Xu L, Xuan A: PI3K/AKT/mTOR signaling mediates valproic acid-induced neuronal differentiation of neural stem cells through epigenetic modifications. *Stem Cell Reports* 2017; 8:1256–69
  25. Wang C, Wang X, Su Z, Fei H, Liu X, Pan Q: The novel mTOR inhibitor Torin-2 induces autophagy and downregulates the expression of UHRF1 to suppress hepatocarcinoma cell growth. *Oncol Rep* 2015; 34:1708–16
  26. Moyon S, Huynh JL, Dutta D, Zhang F, Ma D, Yoo S, Lawrence R, Wegner M, John GR, Emery B, Lubetzki C, Franklin RJM, Fan G, Zhu J, Dupree JL, Casaccia P: Functional characterization of DNA methylation in the oligodendrocyte lineage. *Cell Rep* 2016; 15:748–60
  27. Moyon S, Ma D, Huynh JL, Coutts DJC, Zhao C, Casaccia P, Franklin RJM: Efficient remyelination requires DNA methylation. *eNeuro* 2017; 4:ENEURO.0336-16.2017
  28. Moyon S, Casaccia P: DNA methylation in oligodendroglial cells during developmental myelination and in disease. *Neurogenesis (Austin)* 2017; 4:e1270381
  29. Zhou M, Li W, Huang S, Song J, Kim JY, Tian X, Kang E, Sano Y, Liu C, Balaji J, Wu S, Zhou Y, Zhou Y, Parivash SN, Ehninger D, He L, Song H, Ming GL, Silva AJ: mammalian target of rapamycin inhibition ameliorates cognitive and affective deficits caused by Disc1 knockdown in adult-born dentate granule neurons. *Neuron* 2013; 77:647–54
  30. Assinck P, Duncan GJ, Plemel JR, Lee MJ, Stratton JA, Manesh SB, Liu J, Ramer LM, Kang SH, Bergles DE, Biernaskie J, Tetzlaff W: Myelinogenic plasticity of oligodendrocyte precursor cells following spinal cord contusion injury. *J Neurosci* 2017; 37:8635–54
  31. Preston AR, Eichenbaum H: Interplay of hippocampus and prefrontal cortex in memory. *Curr Biol* 2013; 23:R764–73
  32. Frankland PW, Bontempi B: The organization of recent and remote memories. *Nat Rev Neurosci* 2005; 6:119–30
  33. Fields RD: Neuroscience. Myelin—More than insulation. *Science* 2014; 344:264–6
  34. Sacco R, Biseco A, Corbo D, Della Corte M, d'Ambrosio A, Docimo R, Gallo A, Esposito F, Esposito S, Cirillo M, Lavorgna L, Tedeschi G, Bonavita S: Cognitive impairment and memory disorders in relapsing-remitting multiple sclerosis: The role of white matter, gray matter and hippocampus. *J Neurol* 2015; 262:1691–7
  35. Damjanovic D, Valsasina P, Rocca MA, Stromillo ML, Gallo A, Enzinger C, Hulst HE, Rovira A, Muhlert N, De Stefano N, Biseco A, Fazekas F, Arévalo MJ, Yousry TA, Filippi M: Hippocampal and deep gray matter nuclei atrophy is relevant for explaining cognitive impairment in MS: A multicenter study. *AJNR Am J Neuroradiol* 2017; 38:18–24
  36. Chen BH, Park JH, Lee TK, Song M, Kim H, Lee JC, Kim YM, Lee CH, Hwang IK, Kang IJ, Yan BC, Won MH, Ahn JH: Melatonin attenuates scopolamine-induced cognitive impairment via protecting against demyelination through BDNF-TrkB signaling in the mouse dentate gyrus. *Chem Biol Interact* 2018; 285:8–13
  37. Brambrink AM, Back SA, Riddle A, Gong X, Moravec MD, Dissen GA, Creeley CE, Dikranian KT, Olney JW: Isoflurane-induced apoptosis of oligodendrocytes in the neonatal primate brain. *Ann Neurol* 2012; 72:525–35
  38. Jiang D, Lim S, Kwak M, Ryu YK, Mintz CD: The changes of oligodendrocytes induced by anesthesia during brain development. *Neural Regen Res* 2015; 10:1386–7
  39. Stevens B, Porta S, Haak LL, Gallo V, Fields RD: Adenosine: A neuron–glial transmitter promoting myelination in the CNS in response to action potentials. *Neuron* 2002; 36:855–68
  40. Barres BA, Raff MC: Proliferation of oligodendrocyte precursor cells depends on electrical activity in axons. *Nature* 1993; 361:258–60
  41. Gibson EM, Purger D, Mount CW, Goldstein AK, Lin GL, Wood LS, Inema I, Miller SE, Bieri G, Zuchero JB, Barres BA, Woo PJ, Vogel H, Monje M: Neuronal activity

- promotes oligodendrogenesis and adaptive myelination in the mammalian brain. *Science* 2014; 344:1252304
42. Kukley M, Capetillo-Zarate E, Dietrich D: Vesicular glutamate release from axons in white matter. *Nat Neurosci* 2007; 10:311–20
  43. Redondo C, López-Toledano MA, Lobo MV, Gonzalo-Gobernado R, Reimers D, Herranz AS, Paíno CL, Bazán E: Kainic acid triggers oligodendrocyte precursor cell proliferation and neuronal differentiation from striatal neural stem cells. *J Neurosci Res* 2007; 85:1170–82
  44. Grasshoff C, Antkowiak B: Effects of isoflurane and enflurane on GABAA and glycine receptors contribute equally to depressant actions on spinal ventral horn neurones in rats. *Br J Anaesth* 2006; 97:687–94
  45. Petrenko AB, Yamakura T, Sakimura K, Baba H: Defining the role of NMDA receptors in anesthesia: Are we there yet? *Eur J Pharmacol* 2014; 723:29–37
  46. Baumgart JP, Zhou ZY, Hara M, Cook DC, Hoppa MB, Ryan TA, Hemmings HC Jr: Isoflurane inhibits synaptic vesicle exocytosis through reduced Ca<sup>2+</sup> influx, not Ca<sup>2+</sup>-exocytosis coupling. *Proc Natl Acad Sci U S A* 2015; 112:11959–64
  47. Jacinto E, Loewith R, Schmidt A, Lin S, Rüegg MA, Hall A, Hall MN: Mammalian TOR complex 2 controls the actin cytoskeleton and is rapamycin insensitive. *Nat Cell Biol* 2004; 6:1122–8
  48. Wahl SE, McLane LE, Bercury KK, Macklin WB, Wood TL: Mammalian target of rapamycin promotes oligodendrocyte differentiation, initiation and extent of CNS myelination. *J Neurosci* 2014; 34:4453–65
  49. Guardiola-Diaz HM, Ishii A, Bansal R: Erk1/2 MAPK and mTOR signaling sequentially regulates progression through distinct stages of oligodendrocyte differentiation. *Glia* 2012; 60:476–86
  50. Tyler WA, Gangoli N, Gokina P, Kim HA, Covey M, Levison SW, Wood TL: Activation of the mammalian target of rapamycin (mTOR) is essential for oligodendrocyte differentiation. *J Neurosci* 2009; 29:6367–78
  51. Narayanan SP, Flores AI, Wang F, Macklin WB: Akt signals through the mammalian target of rapamycin pathway to regulate CNS myelination. *J Neurosci* 2009; 29:6860–70
  52. Jiang M, Liu L, He X, Wang H, Lin W, Wang H, Yoon SO, Wood TL, Lu QR: Regulation of PERK-eIF2 $\alpha$  signalling by tuberous sclerosis complex-1 controls homeostasis and survival of myelinating oligodendrocytes. *Nat Commun* 2016; 7:12185
  53. Scholl T, Mühlebner A, Ricken G, Gruber V, Fabing A, Samuelli S, Gröppel G, Dorfer C, Czech T, Hainfellner JA, Prabowo AS, Reinten RJ, Hoogendijk L, Anink JJ, Aronica E, Feucht M: Impaired oligodendroglial turnover is associated with myelin pathology in focal cortical dysplasia and tuberous sclerosis complex. *Brain Pathol* 2017; 27:770–80
  54. Carson RP, Kelm ND, West KL, Does MD, Fu C, Weaver G, McBrier E, Parker B, Grier MD, Ess KC: Hypomyelination following deletion of Tsc2 in oligodendrocyte precursors. *Ann Clin Transl Neurol* 2015; 2:1041–54
  55. Figlia G, Norrmén C, Pereira JA, Gerber D, Suter U: Dual function of the PI3K-Akt-mammalian target of rapamycinC1 axis in myelination of the peripheral nervous system. *eLife* 2017; 6:e29241
  56. Lebrun-Julien F, Bachmann L, Norrmén C, Trötz Müller M, Köfeler H, Rüegg MA, Hall MN, Suter U: Balanced mTORC1 activity in oligodendrocytes is required for accurate CNS myelination. *J Neurosci* 2014; 34:8432–48
  57. Dalla Massara L, Osuru HP, Oklopčić A, Milanović D, Joksimović SM, Caputo V, DiGruccio MR, Ori C, Wang G, Todorović SM, Jevtović-Todorović V: General anesthesia causes epigenetic histone modulation of c-Fos and brain-derived neurotrophic factor, target genes important for neuronal development in the immature rat hippocampus. *ANESTHESIOLOGY* 2016; 124:1311–27